2009

Human Dna2 is a nuclear and mitochondrial DNA maintenance protein

Julien P. Duxin
Tampere University Hospital, Finland

Benjamin Dao
Tampere University Hospital, Finland

Peter Martinsson
Tampere University Hospital, Finland

Nina Rajala
Tampere University Hospital, Finland

Lionel Guittat
Tampere University Hospital, Finland

See next page for additional authors

Human Dna2 Is a Nuclear and Mitochondrial DNA Maintenance Protein

Julien P. Duxin, Benjamin Dao, Peter Martinsson, Nina Rajala, Lionel Guittat, Judith L. Campbell, Johannes N. Spelbrink and Sheila A. Stewart

Mol. Cell. Biol. **2009, 29(15):4274. DOI: 10.1128/MCB.01834-08.**
Published Ahead of Print 1 June 2009.

MOLECULAR AND CELLULAR BIOLOGY, Aug. 2009, p. 4274–4282 Vol. 29, No. 15
0270-7306/09/$08.00+0 doi:10.1128/MCB.01834-08

Human Dna2 Is a Nuclear and Mitochondrial DNA Maintenance Protein▽†

Julien P. Duxin,[1] Benjamin Dao,[1] Peter Martinsson,[2] Nina Rajala,[2] Lionel Guittat,[1]# Judith L. Campbell,[3] Johannes N. Spelbrink,[2]* and Sheila A. Stewart[1,4]*

Department of Cell Biology and Physiology[1] and Institute of Medical Technology and Tampere University Hospital,[2] Tampere, Finland; Braun Laboratories, California Institute of Technology, Pasadena, California[3]; and Department of Medicine, Washington University School of Medicine, St. Louis, Missouri 63110[4]

Received 2 December 2008/Returned for modification 5 January 2009/Accepted 20 May 2009

Dna2 is a highly conserved helicase/nuclease that in yeast participates in Okazaki fragment processing, DNA repair, and telomere maintenance. Here, we investigated the biological function of human Dna2 (hDna2). Immunofluorescence and biochemical fractionation studies demonstrated that hDna2 was present in both the nucleus and the mitochondria. Analysis of mitochondrial hDna2 revealed that it colocalized with a subfraction of DNA-containing mitochondrial nucleoids in unperturbed cells. Upon the expression of disease-associated mutant forms of the mitochondrial Twinkle helicase which induce DNA replication pausing/stalling, hDna2 accumulated within nucleoids. RNA interference-mediated depletion of hDna2 led to a modest decrease in mitochondrial DNA replication intermediates and inefficient repair of damaged mitochondrial DNA. Importantly, hDna2 depletion also resulted in the appearance of aneuploid cells and the formation of internuclear chromatin bridges, indicating that nuclear hDna2 plays a role in genomic DNA stability. Together, our data indicate that hDna2 is similar to its yeast counterpart and is a new addition to the growing list of proteins that participate in both nuclear and mitochondrial DNA maintenance.

DNA damage arises from errors in the replication process, as well as a myriad of intrinsic and extrinsic DNA-damaging agents that continually assault cells. Failure to efficiently repair DNA lesions leads to accumulation of mutations that contribute to numerous pathologies, including carcinogenesis. In addition to genomic DNA, mitochondrial DNA (mtDNA) is subject to damage that requires repair to maintain integrity. For these reasons, it is not surprising that DNA replication and repair proteins display significant plasticity that allows participation in several divergent replication and repair processes. In addition, numerous mechanisms, including alternative splicing, posttranslational modifications, or utilization of alternative translation initiation start sites, allow DNA replication and repair proteins such as Pif1, DNA ligase III, and APE1 to localize to the nucleus and the mitochondrion and participate in DNA replication and/or repair (9, 17, 25), thus ensuring genomic DNA and mtDNA integrity.

Dna2 is an evolutionarily conserved helicase/nuclease enzyme. Originally discovered in *Saccharomyces cerevisiae*, Dna2 orthologs are found throughout the animal kingdom, including humans (5, 22, 28). Early studies demonstrated that Dna2 functions in concert with Flap endonuclease 1 (FEN1) to remove long DNA flaps that form upon lagging-strand DNA replication (6). However, in contrast to FEN1, Dna2 is an essential gene in yeast, suggesting that other proteins, including FEN1, cannot compensate for its loss in DNA replication or that it possesses functions beyond its role in Okazaki fragment processing. In agreement with this, genetic and biochemical studies have implicated Dna2 in DNA double-strand break (DSB) repair, telomere regulation, and mitochondrial function (8, 10, 15, 26, 38, 44, 45).

Analysis of Dna2 in yeast revealed that it undergoes dynamic cell cycle localization. Dna2 localizes to telomeres during G_1, relocalizes throughout the genome in S phase, and moves back to the telomere during late S/G_2, where it participates in telomere replication and telomerase-dependent telomere elongation (10). Dna2 also leaves the telomere following treatment with bleomycin and localizes to sites of DNA DSBs (10). In addition, *dna2* mutants are sensitive to DNA damage induced by gamma radiation and methanesulfonic acid methyl ester (7, 15). These phenotypes may be explained by recent work demonstrating that Dna2 plays an important role in 5′-end resection following DSBs. Indeed, upon induction of DSBs and initiation of 5′-end resection by the Mre11-Rad50-Xrs2 complex, Dna2 and Sgs1 cooperate to further degrade the 5′ end, creating long 3′ strands essential for homologous recombination (26, 45). Finally, while *dna2*Δ mutations are lethal in budding yeast, the *dna2*Δ *pif1-m2* (nuclear PIF1) double mutations rescue *dna2*Δ lethality but produce a petite phenotype, suggesting that Dna2 is also involved in mtDNA maintenance (8).

Recently, the human ortholog of Dna2 was cloned and characterized (23, 29). Biochemical analysis revealed that, similar to its yeast counterpart, the human Dna2 (hDna2) protein possesses nuclease, ATPase, and limited helicase activities (23,

* Corresponding author. Mailing address for Sheila A. Stewart: Department of Cell Biology and Physiology, Washington University School of Medicine, 660 South Euclid Avenue, Campus Box 8228, St. Louis, MO 63110. Phone: (314) 362-7437. Fax: (314) 362-7463. E-mail: sheila.stewart@cellbiology.wustl.edu. Mailing address for Johannes N. Spelbrink: Institute of Medical Technology, FI-33014 University of Tampere, Tampere, Finland. Phone: 358 3 3551 8598. Fax: 358 3 3551 7710. E-mail: hans.spelbrink@uta.fi.

Present address: INSERM U565, CNRS UMR 5153, USM 503 Muséum National d'Histoire Naturelle, Paris, France.

† Supplemental material for this article may be found at http://mcb.asm.org/.

▽ Published ahead of print on 1 June 2009.

29), suggesting that it carries out analogous functions in yeast and mammalian cells. However, hDna2's putative role in genomic DNA repair and replication was called into question by a recent study suggesting that hDna2 is absent from the nucleus and found exclusively within the mitochondria, where it participates in mtDNA repair (44). Further in vitro biochemical studies suggested that hDna2 also participates in mtDNA replication (44). Here, we confirm that hDna2 localizes to the mitochondria and demonstrate that hDna2 participates in mtDNA replication and repair. However, our studies go further by uncovering a nuclear form of hDna2 that plays an important role in genomic stability. Indeed, we demonstrate that depletion of hDna2 leads to the appearance of aneuploid cells and the formation of internuclear chromatin bridges, indicating that hDna2, like its yeast counterpart, is essential to maintain nuclear DNA stability.

MATERIALS AND METHODS

Cell culture. Unless otherwise indicated, cells were incubated at 37°C in 5% CO_2. HeLa and HEK293 cells were cultured in Dulbecco's modified Eagle's medium (DMEM; Sigma, St. Louis, MO) containing 10% fetal bovine serum (FBS) and 1% penicillin-streptomycin. Primary human BJ fibroblasts were cultured in DMEM and M199 (4:1; Sigma, St. Louis, MO) containing 15% FBS and 1% penicillin-streptomycin. Stable cell lines expressing wild-type and various inducible mutant forms of Twinkle were created as described previously (40) by using the Flp-In T-Rex 293 host cell line (Invitrogen, Carlsbad, CA). The resulting cells were grown in DMEM (Sigma, St. Louis, MO) supplemented with 10% FBS (Sigma, St. Louis, MO), 2 mM L-glutamine, 150 μg/ml hygromycin, and 15 μg/ml blasticidin in a 37°C incubator at 8.5% CO_2. The U2OS and 143B osteosarcoma cell lines were similarly maintained but in the absence of selection antibiotics.

Virus production and infection. Virus production and infections were carried out as described previously (32). Briefly, 293T cells were transfected by using TransIT-LT1 (Mirus, Madison, WI). Virus was collected 48 h posttransfection, and infections were carried out in the presence of 10 μg/ml of protamine sulfate. At 48 h postinfection, target cells were selected with 2 μg/ml puromycin. The pLKO.1 shDna2, pResQ shDna2′, and pLKO.1 shSCR lentiviruses were produced by cotransfection with pCMVΔR8.2 and pCMV-VSV-G (8:1 ratio). The sequence used for shDna2 was 5′-CATAGCCAGTAGTATTCGATG-3′, that used for shDna2′ was 5′-GCAGTATCTCCTCTAGCTAGT-3′, and that used for shSCR was previously reported (32). For fractionation experiments, HEK293 and HeLa 1.2.11 cells were transfected on 10-cm plates with a mixture of three Stealth small interfering RNA duplex oligonucleotides (DNA2HSS 141856, 141857, and 141858; Invitrogen) against hDna2, at 800 pmol each, by using Lipofectamine 2000 according the manufacturer's protocol. As a negative control, we used a Stealth Universal negative control (12935-200; Invitrogen). Cells were isolated and processed for subcellular fractionation at 48 h following transfection.

Immunoprecipitation and Western blot analysis. Cells were washed in phosphate-buffered saline (PBS), lysed in buffer H-500 (50 mM HEPES [pH 7.4], 500 mM NaCl, 10% glycerol, 1 mM dithiothreitol, 1 mM EDTA, 0.5% Nonidet P-40, aprotinin, leupeptin, pepstatin, and phenylmethylsulfonyl fluoride), and sonicated (three cycles of a 30-s pulse and a 30-s cooling interval) (23). Cell extracts were dialyzed overnight with H-100 (50 mM HEPES [pH 7.4], 100 mM NaCl, 10% glycerol, 1 mM dithiothreitol, 1 mM EDTA, 0.5% Nonidet P-40), and 1 mg of lysate was immunoprecipitated. Cellular extracts were precleared for 2 h with 20 μl of protein A beads (Amersham, Amersham, United Kingdom) and incubated with 5 μg of hDna2 antibody (42439; Abcam, Cambridge, MA) or immunoglobulin (IgG; Sigma, St. Louis, MO) overnight. Bound protein was eluted and analyzed by 8% sodium dodecyl sulfate-polyacrylamide gel electrophoresis, and Western blot analysis was carried with the hDna2 antibody (42439; Abcam, Cambridge, MA). All protein concentrations were measured by using the Bradford assay (3).

Mitochondrial and subcellular fractionations. Crude mitochondrial fractions of all cell lines were obtained and validated as previously described (12). In brief, cells were homogenized by hypotonic swelling and Dounce homogenization. The homogenized sample was centrifuged at 800 × *g* at 4°C for 5 min to pellet the nuclear fraction. The centrifugation was repeated, and the resulting supernatant was centrifuged at 12,000 × *g* at 4°C for 10 min to obtain a mitochondrial pellet. The mitochondrial pellet was again centrifuged with fresh homogenization buffer and lysed either directly in sample buffer or with the addition of 50 mM Tris HCl (pH 7.5), 150 mM NaCl, 1 mM EDTA, and 1% Triton X-100 in the presence of protease inhibitors (Roche). The crude nuclear pellet obtained from the initial cell lysis was further purified with an Optiprep gradient and processed as previously described (12). All protein concentrations were measured by using the Bradford assay (3).

Proteinase K protection assay. We used Proteinase K protection assays to more precisely determine the localization of hDna2 within mitochondria. For this purpose, HEK293 cell mitochondria were isolated as described above. Mitoplasts were made by permeabilizing the outer mitochondrial membrane with a digitonin (50% high-pressure liquid chromatography pure) solution using a fixed final ratio (ratio of micrograms of digitonin to micrograms of mitochondria = 0.4). Digitonin was made fresh prior to each experiment by dissolving 50% high-pressure liquid chromatography pure digitonin (Sigma, St. Louis, MO) in PBS (with protease inhibitors). The degree of permeabilization and, more particularly, lack of inner membrane permeabilization during mitoplast isolation were verified by immunoblotting the final submitochondrial fractions with antibodies against known endogenous proteins, including CoxII and TFAM. Mitochondria and mitoplasts were washed once with protease inhibitor-free PBS and treated with proteinase K (100 μg/ml) in the absence or presence of 0.5% Triton X-100 for 15 min at 4°C. The reaction was terminated by the addition of 10 mM (final concentration) phenylmethylsulfonyl fluoride (in ethanol), an equal volume of 2× sample buffer was added, and the sample was immediately placed at 95°C for heat denaturation prior to Western blot analysis. Western blot analyses of cell and mitochondrial subfractions and proteinase K protection assays used antibodies against hDna2 (42439; Abcam, Cambridge, MA), γ-actin (NB 600 533; Novus Biologicals, Littleton, CO), nucleophosmin (32-5200; Invitrogen), and TFAM (kind gift of Rudolf Wiesner).

Immunofluorescence microscopy. HeLa, HEK293, U2OS, 143B, and BJ cells were grown for 1 to 2 days on coverslips, and Flp-In T-Rex 293 cells were grown on poly-L-lysine-coated coverslips. Cells were then washed in PBS and fixed in 3.7% paraformaldehyde, permeabilized in 0.5% Triton X-100, and treated with blocking buffer (10% FBS, 2% goat serum, 0.2% Tween 20) at room temperature. Antibodies were diluted in blocking buffer and incubated with cells for 1 h at room temperature. Cells were washed in PBS containing 0.02% Tween 20 and mounted with 4′,6-diamidino-2-phenylindole (DAPI). For transient transfection of Twinkle expression constructs, TransIT-LT1 (Mirus, Madison, WI) was used. Induction of expression of Twinkle variants using Flp-In T-Rex 293 cells was done 2 days prior to immunofluorescence detection with the indicated amounts of doxycycline. Immunofluorescence detection was carried out with a polyclonal hDna2 antibody (42439; Abcam, Cambridge, MA) or Alexa-Fluor 488-conjugated bromodeoxyuridine (BrdU) monoclonal antibody (A21303; Invitrogen, Carlsbad, CA) as the primary antibody. The secondary antibody was anti-rabbit IgG–Alexa-Fluor 488 or 546 (Invitrogen, Carlsbad, CA). Detection of nucleoids by immunofluorescence was otherwise done as described previously (12) using IgM anti-DNA monoclonal antibody AC-30-10 (PROGEN, Shingle Springs, CA), a monoclonal c-myc IgG antibody (Roche, Indianapolis, IN), or a polyclonal hDna2 antibody (42439; Abcam, Cambridge, MA) as the primary antibody. The secondary antibody was anti-mouse IgG–Alexa-Fluor 488 or 568 (Invitrogen, Carlsbad, CA, myc), anti-mouse IgM–Alexa-Fluor 488 or 568 (DNA), or anti-rabbit IgG–Alexa-Fluor 488 or 568 (hDna2). Images were acquired with an LSM510 confocal microscope (Carl Zeiss, Thornwood, NY). Images were processed with Photoshop 7.0 (Adobe, San Jose, CA). Colocalization images were generated by using the calculator function in Photoshop CS2 on the RGB merged color image. Similar images were also obtained with a colocalization plug-in in ImageJ (not shown). The specificity of the hDna2 antibody in BJ cells was confirmed by coincubating hDna2 antibody with a specific blocking peptide (42548; Abcam, Cambridge, MA) at a 1:500 dilution.

Two-dimensional agarose gel electrophoresis. Mitochondrial nucleic acids were extracted as previously described (42) from short hairpin RNA-infected HEK293 cells. Purified mtDNA was digested with HincII and separated by two-dimensional neutral/neutral agarose gel electrophoresis (2DNAGE) as previously described (4, 16, 40). Equal loading was verified by ethidium bromide staining. Gels were transferred to a nucleic acid membrane and hybridized with a ^{32}P-labeled probe for human mtDNA (nucleotides 14983 to 15593). DNA replication intermediates were quantitated by scanning the 2DNAGE gels and normalizing them to the 1n spot of a shorter exposure by using the measuring function in ImageJ. Briefly, boxes were drawn around ribonucleotide incorporation throughout the lagging strand (RITOLS) structures, X spikes, y arcs, bubble arcs (long exposure), and 1n spots (shorter exposure). Each value was first normalized to the 1n spot, added, and then normalized to the shSCR samples.

An overall 20% reduction in mitochondrial replication intermediates was observed upon hDna2 depletion averaging two different independent experiments.

mtDNA damage assay. Short hairpin RNA-infected HeLa cells were seeded at 10^6/10-mm culture plate and incubated overnight at 37°C. The next morning, cells were washed once with PBS and treated with 2 mM H_2O_2 in medium at 37°C for 30 min. Cells were either immediately harvested or allowed to recover in DMEM plus 10% FBS for 1, 2, or 24 h. Total cellular DNA was extracted with a genomic DNA extraction kit (Qiagen, Valencia, CA).

Quantification of mtDNA damage was done by a quantitative PCR (qPCR) that amplifies long DNA targets as previously described (33). Briefly, the following primers were used to amplify an 8.9-kb fragment of mtDNA: 5′-TCTA AGCCTCCTTATTCGAGCCGA-3′ (sense) and 5′-TTTCATCATGCGGAGA TGTTGGA-3′ (antisense). A 221-bp fragment of mtDNA was also amplified to normalize to the copy number of the mitochondrial genome present: 5′-CCCC ACAAACCCCATTACTAAACCCA-3′ (sense) and 5′-TTTCATCATGCGGA GATGTTGGA-3′ (antisense). The relative PCR product was calculated by dividing the fluorescence value of the treated samples by that of the untreated sample. Quantification of genomic DNA damage was done with a qPCR that amplifies a 13.5-kb fragment of the β-globin gene. The primers used to amplify the β-globin gene were 5′-CGAGTAAGAGACCATTGTGGCAG-3′ (sense) and 5′-GCACTGGCTTTAGGAGTTGGACT-3′ (antisense). The relative PCR product was normalized to the copy number of the mitochondrial genome.

Internuclear chromatin bridge assay. hDna2 knockdown and control U2OS and HeLa cells were seeded into a 12-well plate at 5×10^4 cells per well 5 days postinfection. Twenty-four hours later, cells were fixed and stained with DAPI. The number of internuclear bridges was quantified in relation to the total number of nuclei. At least 1,000 nuclei were counted per well, and six wells were counted for each sample. Images were processed with Photoshop 7.0 by using the gray scale and invert function (Adobe, San Jose, CA).

Growth curve. hDna2 knockdown and control U2OS cells were seeded into six-well plates at 7.5×10^4 per well, in triplicate, at 5 days postinfection. Cells were lifted and counted at 24, 48, and 72 h after seeding.

Flow-activated cell sorting analysis. U2OS and HeLa cells were seeded at 1×10^6 per 10-cm plate at 5 days postinfection. Twenty-four to 48 h later, cells were lifted, stained with hypotonic propidium iodide, and subjected to fluorescence-activated cell sorting analysis to determine DNA content as previously described (36).

RESULTS

hDna2 localizes to the nucleus and cytoplasm. Yeast Dna2 is found at telomeres during the G_1 phase of the cell cycle and relocalizes to sites of DNA replication during S phase (10). In addition, when cells are treated with DNA-damaging agents such as bleomycin, Dna2 transits from telomeres to sites of DNA damage (7, 10). This dramatic redistribution of Dna2 suggests that in yeast, Dna2 plays roles in both DNA replication and repair. To characterize the biological functions of Dna2 in human cells, we first set out to establish whether it displayed a similar dynamic subcellular localization. As expected, we noted the presence of hDna2 in the nuclei of a variety of cell types (including BJ, HeLa, HEK293, U2OS, and 143B cells), albeit to various degrees (Fig. 1A). Primary human BJ fibroblasts displayed the most robust hDna2 nuclear staining of the cell lines analyzed (Fig. 1A). In addition to the nuclear staining, we also observed a robust punctate hDna2 pattern within the cytoplasm (Fig. 1A). To control for the specificity of our antibody and demonstrate that the cytoplasmic and nuclear hDna2 signals were real, we depleted hDna2 from HeLa cells by RNA interference (RNAi). Upon depletion of hDna2, both the nuclear and cytoplasmic hDna2 foci were significantly reduced (Fig. 1B). Because we were unable to achieve significant hDna2 knockdown in BJ fibroblasts, which displayed the most robust nuclear hDna2 signal, we utilized blocking peptides to demonstrate that the cytoplasmic and nuclear hDna2 signals in BJ cells were lost, indicating that

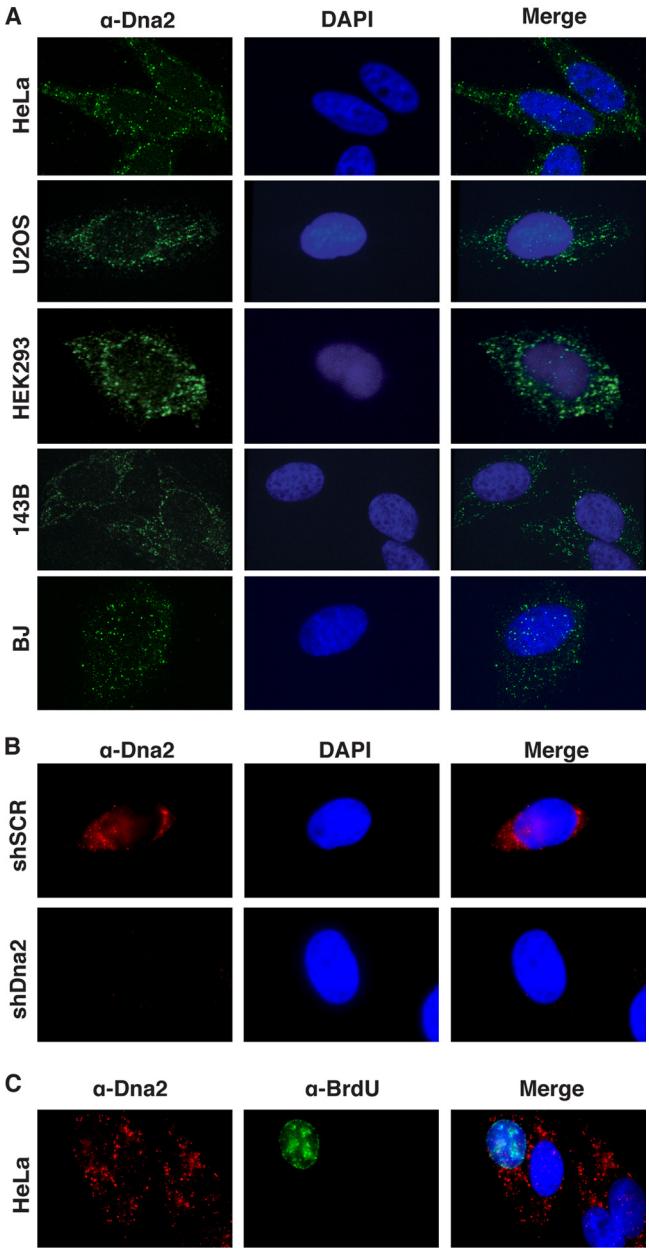

FIG. 1. hDna2 localizes within the cytoplasm and the nucleus. (A) Representative image of confocal immunofluorescence staining of hDna2 in HeLa, U2OS, HEK293, and 143B cells and primary BJ fibroblasts. hDna2 was stained with a polyclonal antibody targeting the hDna2 C terminus (green), while nuclei were stained with DAPI (blue). (B) Representative image of immunofluorescence staining of hDna2 in HeLa cells infected with a short hairpin targeting hDna2 (shDna2, bottom) versus a control hairpin (shSCR, top). (C) Immunofluorescence images of replicating HeLa cells stained for hDna2. Cells were grown in the presence of BrdU for 1 h and stained for hDna2 (red) and BrdU (green).

the immunofluorescence signal was specific (see Fig. S1 in the supplemental material). Taken together, our data indicate that cytoplasmic and nuclear forms of hDna2 exist in the cell.

In primary BJ fibroblasts, we observed more-robust nuclear hDna2, while analysis of HeLa cells revealed that hDna2 was predominantly cytoplasmic. To determine whether most of the

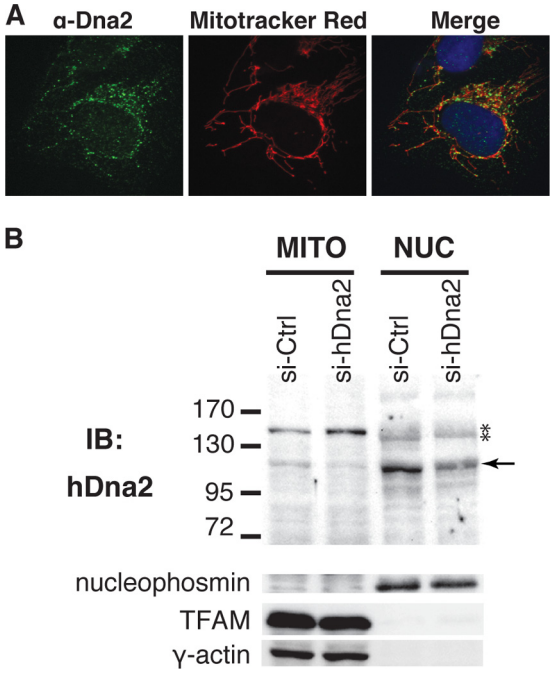

FIG. 2. hDna2 localizes to the mitochondria and nucleus. (A) Confocal immunofluorescence images of U2OS cells showing hDna2 (green) and mitochondria (red) labeled with MitoTracker. Note the punctate nuclear staining of hDna2. (B) Subcellular fractionation of HEK293 cells following transduction with synthetic RNAs targeting hDna2 mRNA. Mitochondrial (MITO) and nuclear (NUC) fractions were resolved by 7.5% sodium dodecyl sulfate-polyacrylamide gel electrophoresis and probed with the hDna2 antibody. Controls (Ctrl) for the mitochondrial and nuclear fractions were TFAM and nucleophosmin, respectively. The arrow indicates hDna2, and the asterisks denote nonspecific bands. IB, immunoblot. The values on the left are molecular sizes in kilodaltons.

hDna2 was retained in the cytoplasm during interphase and localized to the nucleus upon entrance into S phase, we incubated HeLa cells with BrdU for 1 h. As shown in Fig. 1C, hDna2 did not relocalize to the nuclei of HeLa cells actively undergoing DNA replication, suggesting that the limited nuclear fraction of hDna2 is sufficient to participate in replication (Fig. 1A and 2B).

hDna2 localizes to the mitochondria. In yeast, Dna2 is a nuclease/helicase enzyme that functions in the nucleus but is also implicated in mtDNA maintenance (8). The existence of cytoplasmic Dna2 raised the possibility that it localizes to the mitochondria and participates in mtDNA replication and/or repair. To determine whether hDna2 localizes to the mitochondria, we utilized a mitochondrion-specific dye, MitoTracker. Osteosarcoma U2OS cells were utilized for these studies because they are flat and contain large cytoplasms and thus allow high resolution of the mitochondria. Upon immunofluorescence analysis of hDna2 in U2OS cells, we observed significant colocalization with MitoTracker (Fig. 2A), indicating that a substantial fraction of cytoplasmic hDna2 is present in the mitochondria. Similar results were obtained in HeLa and HEK293 cells (see Fig. 4; data not shown).

We next utilized subcellular fractionation to confirm our immunofluorescence findings. Analysis of a crude mitochondrial fraction and a highly pure nuclear fraction of HEK293, HeLa, 143B, and U2OS cells revealed the presence of a 120-kDa species of hDna2 within the mitochondria and nucleus (Fig. 2B and data not shown). Importantly, depletion of hDna2 in HEK293 and HeLa cells led to a reduction in both the mitochondrial and nuclear bands, indicating that the ~120-kDa band is hDna2 (Fig. 2B and data not shown). It is unlikely that the nuclear form is the result of cytosolic contamination of the nuclear fraction because we did not detect cytoplasmic γ-actin in the nuclear fraction, whereas we did observe it in the crude mitochondrial fractions (Fig. 2B) and cytosolic fractions (data not shown). Similarly, we did not observe any appreciable mitochondrial contamination in our nuclear preparation (see TFAM control). Together, these results support our immunofluorescence analysis and indicate that hDna2 localizes to both the nucleus and the mitochondria.

hDna2's presence in the mitochondria raised the possibility that it plays a role in the replication and/or repair of mtDNA. Therefore, we next sought to determine whether hDna2 colocalizes with mtDNA. Immunofluorescence analysis of hDna2 and mtDNA revealed that they were often in close juxtaposition and frequently showed overlap in their signals (Fig. 3A). This result was confirmed by further coimmunofluorescence experiments with the mitochondrial helicase Twinkle (Fig. 3B). mtDNA is packed into nucleoprotein complexes referred to as nucleoids, and the Twinkle helicase localizes to these structures (18, 35). Colocalization experiments with cells transduced with enhanced green fluorescent protein (EGFP)-tagged Twinkle revealed a modest degree of overlap in the Twinkle and hDna2 signals (Fig. 3B), further demonstrating that hDna2 localizes to nucleoids in a subset of mitochondria.

The limited colocalization of hDNA2 with mtDNA raised the possibility that hDNA2 localizes within the mitochondria but is excluded from the majority of nucleoids or that most of the hDNA2 is situated in the outer membrane or intermembrane space of mitochondria. To distinguish between these possibilities, we carried out a proteinase K protection assay (Fig. 3C). These results showed that in both mitochondria and mitoplasts (with the outer mitochondrial membrane ruptured by digitonin treatment), a small fraction of hDna2 was protected from proteinase K degradation. However, hDna2 was degraded in the presence of the detergent Triton X-100, illustrating the efficiency of the proteinase K treatment. As expected, TFAM, also a nucleoid protein, showed a pattern of proteinase K protection similar to that of hDna2, but more of the protein was protected. These data indicate that at least a subfraction of hDna2 is found in the same mitochondrial compartment (inner membrane and/or matrix) as other nucleoid proteins.

hDna2 associates with mtDNA in the presence of mutant Twinkle proteins that induce replication stalling and nucleoid aggregation. Our initial immunofluorescence analysis of hDna2 subcellular localization indicated that only a fraction of hDna2 colocalized with DNA-containing nucleoids. We next questioned whether DNA damage resulting from physiological sources altered hDna2 subcellular localization. Twinkle is a mitochondrion-specific helicase. Point mutations in Twinkle have been identified in patients with progressive external ophthalmoplegia, a mitochondrial disorder associated with accumulation of mtDNA deletions (35, 43). Importantly, expres-

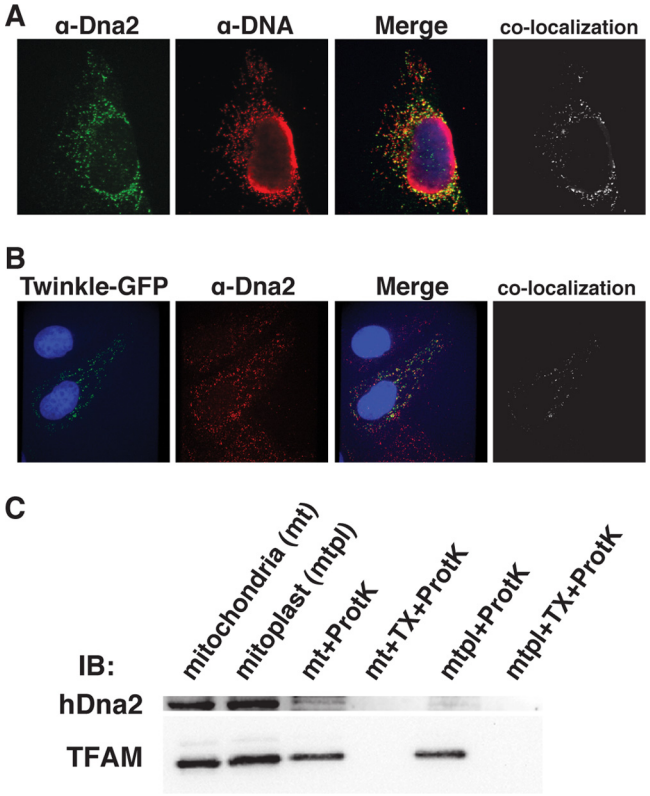

FIG. 3. hDna2 colocalizes with mtDNA. (A) Confocal images showing colocalization of hDna2 (green, left) with mtDNA (red) in U2OS cells. mtDNA was stained with a specific DNA antibody (αDNA). Colocalization is shown in black and white (right). (B) Representative confocal images of U2OS cells transiently transfected with Twinkle-EGFP (green, left) and stained for hDna2 (red). The right part of the panel shows colocalization depicted in black and white. (C) Western blot analysis of hDna2 following mitochondrial subfractionation and proteinase K treatment reveals the presence of hDna2 species within the mitochondria. HEK293 mitochondria were isolated and subfractionated as described in Materials and Methods. Samples were analyzed by immunoblot (IB) analysis with an antibody against hDna2 and reprobed with an antibody against the mitochondrial nucleoid protein TFAM. Approximately 20 μg of mitochondrial extract (mt), typically 3 to 5% of the starting material, was loaded. Mitoplasts (mtpl) were loaded at an equivalent portion of the total volume. Mitochondria (mt) and mitoplasts were left untreated, treated with 100 μg/ml proteinase K (+ProtK) for 15 min at 4°C, or treated with ProtK and Triton X-100 (+TX+ProtK), as indicated.

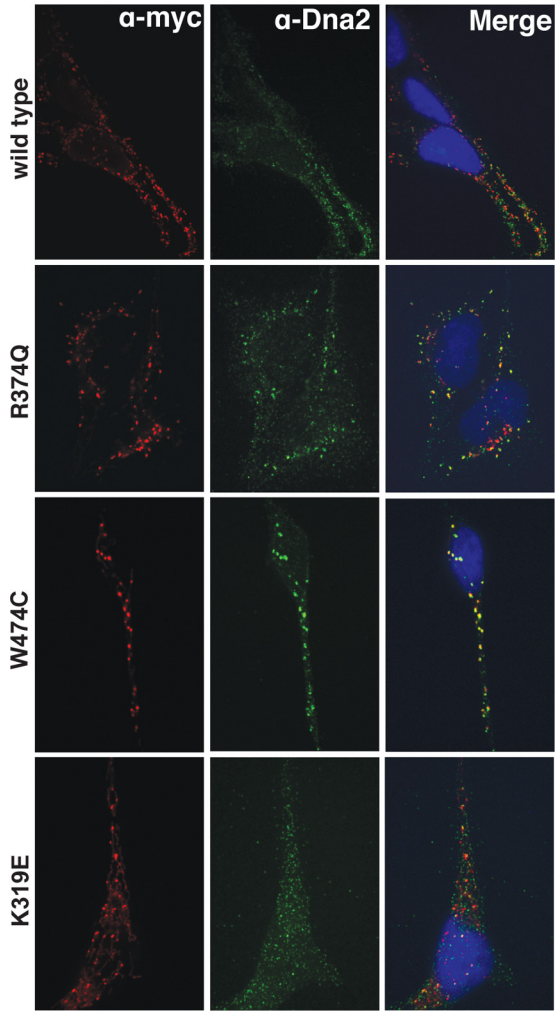

FIG. 4. Colocalization of hDna2 with wild-type and mutant Twinkle proteins. Expression of wild-type Twinkle with a myc epitope tag and R374Q, W474C, and K319E mutant Twinkle proteins with a similar tag was induced in Flp-In T-Rex 293 cells for 2 or 3 days with 3 ng/ml doxycycline. Twinkle proteins were detected by immunofluorescence assay with a myc monoclonal antibody (red), while hDna2 was detected with a rabbit polyclonal antibody (green). Merged images (far right) include the signal detected from staining with DAPI.

sion of mutant Twinkle proteins results in stalling of mtDNA replication forks and loss of mtDNA (19, 40). To address how hDna2 responds to mutant Twinkle protein expression, we utilized inducible HEK293 cell lines expressing either wild-type or mutant Twinkle protein. Importantly, the inducible cell lines allowed us to examine the impact of acute protein expression at nearly physiological levels of Twinkle that have been shown to be sufficient to induce stalled replication forks within mtDNA (19, 40). Induction of wild-type Twinkle expression had little to no detectable impact on hDna2 localization (Fig. 4). In contrast, expression of mutant Twinkle proteins had variable effects on hDna2 localization. The G575D mutation failed to alter hDna2's subcellular localization (data not shown), while both K421A (not shown) and K319E had only a modest effect, producing some nucleoid aggregation and accumulation of hDna2 in a subset of nucleoids. In contrast, expression of R374Q and W474C mutant proteins resulted in a dramatic relocalization of hDna2 to mtDNA nucleoids, indicating that, under some conditions, hDna2 is more permanently associated with nucleoids and illustrating that its partial colocalization under normal conditions is not by chance. This altered hDna2 localization is exemplified by the W474C mutant protein, which showed a faint uniform mitochondrial staining, illustrating that the W474C mutant protein did not result in a collapse or fractionation of the mitochondrial network that might otherwise also explain the hDna2 accumulation with W474C mutant protein-containing nucleoids.

hDna2 depletion abrogates mtDNA repair. Expression of mutant Twinkle proteins known to cause mitochondrial replication fork stalling led to a more pronounced hDna2 nucleoid

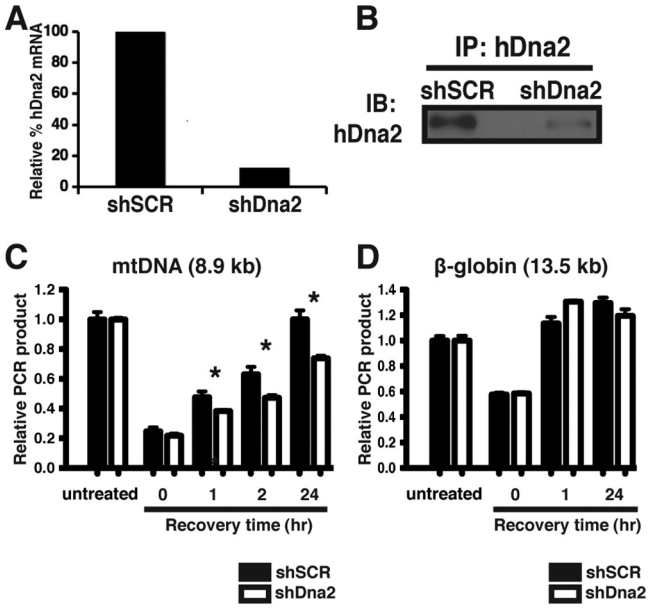

FIG. 5. hDna2 depletion abrogates mtDNA repair. (A) Stable knockdown of hDna2 by virus-based RNAi determined by quantitative reverse transcription-PCR in HeLa cells. Results are normalized to those obtained with the shSCR control cell line. (B) Immunoblot (IB) analysis of hDna2 immunoprecipitation (IP) from HeLa cells stably expressing an shSCR (control) or shDna2 hairpin. (C) Histogram representing mtDNA amplification by qPCR of DNA extracted from HeLa cells expressing shSCR or shDna2. Cells were treated with 2 mM H_2O_2 and allowed to recover for 0, 1, 2, or 24 h. An 8.9-kb mitochondrial PCR product was quantified by PicoGreen and normalized to untreated samples and to the mtDNA copy number determined by the amplification of a 221-bp short mitochondrial fragment. Error bars represent standard errors of PCRs run in quadruplicate for each condition. *, $P < 0.05$. (D) Histogram representing the amplification of a 13.5-kb region of the β-globin gene representing repair of genomic DNA in untreated cells or 0, 1, or 24 h following H_2O_2 treatment.

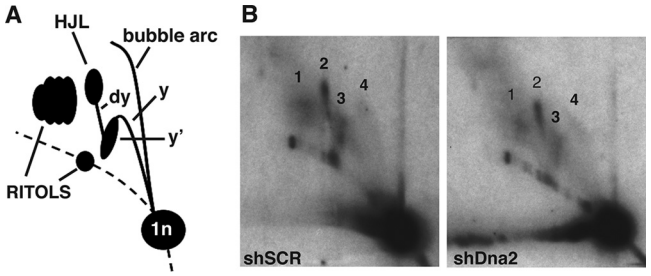

FIG. 6. hDna2 depletion affects the fidelity of mtDNA replication. 2DNAGE analysis of purified mtDNA digested with HincII and probed with a cytochrome *b*-specific fragment. (A) Schematic of 2DNAGE. The abbreviation 1n stands for a 3.9-kb nonreplicating HincII fragment, y and y′ indicate the ascending and descending parts of the y arc, and dy indicates double-Y structures. These will eventually form resolution intermediates resembling Holliday junctions (HJL, Holliday junction-like molecules). (B) 2DNAGE of mtDNA isolated from control cells (left) or cells depleted of hDna2 (65% knockdown of hDna2 mRNA; right). Numbers on the two-dimensional gels: 1, RITOLS; 2, HJL; 3, y′; 4, bubble arc.

localization. This observation raised the possibility that hDna2 contributes to mitochondrial replication and/or repair. To address the role hDna2 plays in mitochondrial function, we utilized virus-mediated RNAi to target hDna2. Introduction of an hDna2 viral RNAi construct into HeLa cells resulted in an ~80% reduction in mRNA and protein levels (Fig. 5A and B). To determine whether hDna2 has an impact on mtDNA repair, we analyzed the kinetics of mtDNA repair upon hDna2 depletion. Cells were treated with 2 mM hydrogen peroxide (H_2O_2) for 30 min to induce oxidative DNA lesions. Because base lesions, abasic sites, and strand breaks interfere with amplification of DNA, long-range PCR can be used to measure the kinetics of mtDNA repair (33). Therefore, to assess mtDNA repair, DNA from cells expressing a control RNAi hairpin or cells expressing a hairpin targeting hDna2 was isolated following H_2O_2 treatment. Lesions in mtDNA were assessed by PCR amplification of an 8.9-kb fragment of mtDNA and normalized to mtDNA copy number by using a shorter mtDNA PCR product (221 bp). As an additional control, a DNA fragment from the nuclear β-globin gene (13.5 kb) was also amplified.

Analysis of mtDNA 0, 1, 2, and 24 h after H_2O_2 treatment revealed that hDna2 depletion resulted in a significant reduction in the repair of oxidative lesions within the mtDNA (Fig. 5C). In contrast, analysis of the nuclear β-globin gene revealed no significant differences in the repair of nuclear DNA (Fig. 5D). However, given that we observed less DNA damage and faster DNA repair kinetics within the nucleus (by 1 h, all of the nuclear β-globin is repaired; compare mtDNA and β-globin for the shSCR sample), this assay does not rule out a role for hDna2 in nuclear DNA repair. Together, these experiments indicate that hDna2 plays an active role in the repair of mtDNA.

hDna2 depletion affects the fidelity of mtDNA replication. In order to determine whether hDna2 participates in mtDNA replication, we utilized 2DNAGE to analyze mitochondrial replication intermediates in cells depleted of hDna2. mtDNA was purified from HEK293 cells and digested with HincII to release a 3.9-kb DNA fragment. Digested mtDNA was run in two dimensions and hybridized with a mitochondrion-specific cytochrome *b* probe (Fig. 6A). As shown in Fig. 6B (right side), depletion of hDna2 led to a moderate yet reproducible decrease in replication intermediates. Indeed, we found a 20% reduction in y arcs, bubble arcs, and RITOLS structures in cells depleted of hDna2 (Fig. 6B, right side) compared to those in control cells (shSCR) (Fig. 6B, left side). This observation indicates that hDna2 depletion leads to reduced mtDNA replication, indicating that hDna2 participates in the replication of mtDNA.

hDna2 is important to maintain nuclear DNA stability. Our original subcellular fractionation and immunofluorescence studies indicated that hDna2 was present in the mitochondria and nucleus. This raised the possibility that hDna2, like its yeast counterpart, is important to maintain both mitochondrial and nuclear DNA stability (8, 10, 15, 26, 38, 45). We next sought to determine if hDna2 participates in genomic DNA maintenance. To address this possibility, we depleted hDna2 from several cell lines and obtained various degrees of knockdown of hDna2 mRNA (~95% knockdown in U2OS cells, 80% in HeLa, 65% in HEK293 cells, and 20% in BJ cells). Given the significant knockdown obtained in U2OS and HeLa cells, we analyzed the impact of hDna2 depletion in these cells. Upon hDna2 depletion, U2OS cells showed a dramatic growth

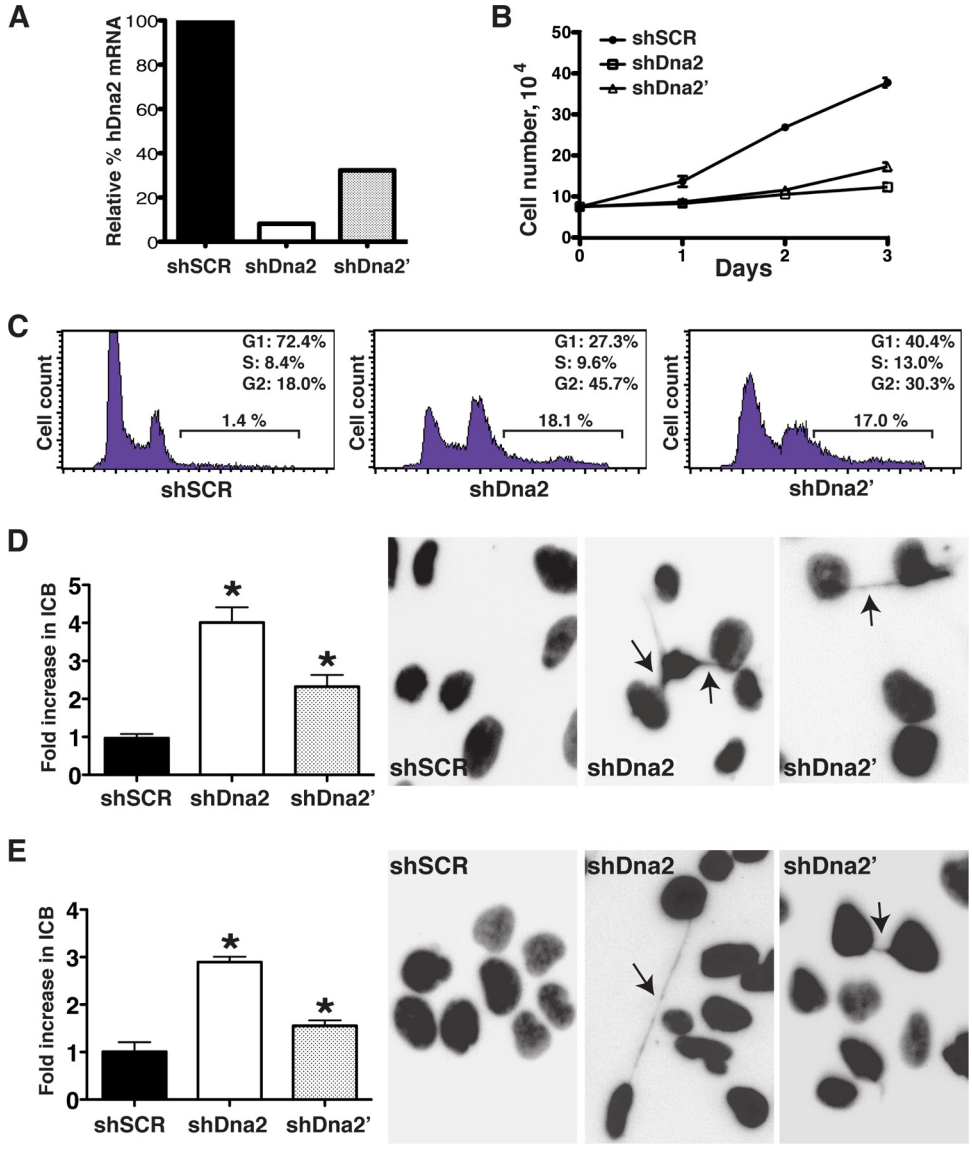

FIG. 7. Depletion of hDna2 leads to nuclear DNA instability. (A) Stable knockdown of hDna2 determined by quantitative reverse transcription-PCR in U2OS cells. Results obtained with two independent hairpins (shDna2 and shDna2′) are normalized to those obtained with the shSCR control cell line. (B) Control U2OS cells or cells depleted of hDna2 were seeded into the wells of a six-well plate at 7.5×10^4 per well in triplicate. Cells were lifted and counted 24, 48, and 72 h after seeding. Error bars represent standard errors of triplicate wells. (C) Fluorescence-activated cytometric analysis of the cell cycle of U2OS cells expressing shDna2, shDna2′, and shSCR. *y* axis, cell count; *x* axis, DNA content. (D) Relative internuclear chromatin bridge (ICB) levels and representative bridges (arrows) following hDna2 depletion in U2OS cells. Results were normalized to those obtained with shSCR. Note that hDna2 depletion was higher in shDna2-transduced cells than in shDna2′-transduced cells. Error bars represent standard errors, and asterisks denote $P < 0.05$. (E) Relative internuclear chromatin bridge levels and representation of HeLa cells following hDna2 depletion. Arrows indicate chromatin bridges. Note that hDna2 depletion in HeLa cells was lower than in U2OS cells.

defect compared to control cells (Fig. 7B). Analysis of DNA content revealed that depletion of hDna2 resulted in an accumulation of cells in the G_2/M phase of the cell cycle and the appearance of aneuploid cells (Fig. 7C). Furthermore, hDna2-depleted cells displayed a significant increase in the appearance of internuclear chromatin bridges (Fig. 7D), indicative of genomic instability. Similar results were obtained with a second independent hDna2 construct (shDNA2′), indicating that neither phenotype was due to an RNAi off-target effect (Fig. 7A to D). In addition, hDna2 depletion in HeLa cells led to similar results, albeit to a lesser extent, consistent with the reduced hDna2 depletion observed in these cells (Fig. 7E). Together, these observations demonstrate that hDna2 plays a role in nuclear DNA stability.

DISCUSSION

In this study, we present immunofluorescence and biochemical evidence for the existence of both nuclear and mitochondrial forms of hDna2. RNAi-directed depletion of hDna2 leads to growth defects, accumulation of aneuploid cells, and the appearance of internuclear chromatin bridges at high fre-

quency, demonstrating a role for hDna2 in genome stability. Moreover, we demonstrate that hDna2 localizes within the mitochondria, where a fraction associates with the mitochondrial inner membrane/matrix. In addition, hDna2 partially colocalizes with the mitochondrion-specific helicase Twinkle, which plays an important role in mtDNA replication. Upon the expression of mutant Twinkle proteins known to cause replication fork stalling and DNA damage, hDna2 accumulates within mtDNA-containing foci, indicating that hDna2 colocalization with mtDNA occurs not by chance but in a temporal/transient fashion to participate in mtDNA replication and/or repair. In support of this, we show that depletion of hDna2 leads to reduced mtDNA repair and replication. Together, these results indicate that hDna2 participates in DNA repair, likely via long patch excision repair and/or homologous recombination (1, 11, 14, 27, 37) and DNA replication within mitochondria.

Our finding that hDna2 participates in mtDNA stability is in agreement with a recent report showing that hDna2 is a mitochondrial repair and replication protein (44). However, our findings differ significantly from this report, which failed to identify nuclear hDna2 and thus suggested that hDna2 differs from its yeast counterpart in regard to a role in nuclear DNA stability. Instead, our findings are in agreement with results obtained with yeast which indicate that Dna2 plays an important role in genomic DNA and mtDNA stability. Indeed, Budd et al. demonstrated that while a *pif1-m2* mutant grows normally on glycerol, a *dna2*Δ *pif1-m2* double mutant displays a petite phenotype indicative of mitochondrial dysfunction (8). Furthermore, yeast Dna2 mutants exhibit defects in telomere stability and DNA repair (10, 38). Again, our studies are in agreement with those done with yeast by showing that hDna2 localizes to the nucleus and that hDna2 depletion results in nuclear DNA instability. While we cannot explain the discordance between the studies with regard to nuclear hDna2, it is important to note that the amount of hDna2 detected by immunofluorescence inside the nucleus fluctuates from cell line to cell line. In addition, the antibodies used in the two studies differ, which may explain the varied localization results.

Our basic understanding of the replication and repair mechanisms that act on mtDNA is rudimentary, but a multitude of proteins localize to the mitochondria and participate in DNA replication and repair. For example, the mitochondrion-specific polymerase γ and helicase Twinkle are important in mtDNA replication and when reconstituted in vitro together with the mitochondrial single-stranded DNA-binding protein function as a minimal mtDNA replisome (24). The importance of Twinkle has been underscored by the discovery of human mutations that lead to mitochondrial diseases, including progressive external ophthalmoplegia (35), mtDNA depletion syndrome (21, 34), and infantile-onset spinocerebellar ataxia (20, 30). In this report, we provide in vivo evidence that hDna2 accumulates within nucleoid structures upon the expression of mutant Twinkle proteins known to induce mtDNA stalling/pausing. Furthermore, we demonstrate that hDna2 is important to ensure efficient mtDNA replication. These observations corroborate results from Zheng et al. which demonstrate that hDna2 directly interacts with polymerase γ and stimulates its polymerase activity in vitro (44). The reduction in mitochondrial replication intermediates in hDna2-depleted cells could indicate that hDna2 is important for initiating mtDNA replication and that the hDna2 helicase activity plays an essential role in this process. Elucidating which hDna2 activity (helicase and/or nuclease) is necessary for efficient mtDNA replication will provide a better understanding of the molecular mechanisms that govern mtDNA replication.

While the Twinkle and polymerase γ proteins localize exclusively to the mitochondria, other proteins with known nuclear functions have also been found within the mitochondria. For example, FEN1, ligase III, and the helicase Pif1 function within the nucleus and mitochondria (17, 25, 27, 31). Investigation of the mechanisms that control the subcellular localization of these proteins revealed that the Pif1 mRNA undergoes differential splicing, producing nuclear and mitochondrial isoforms (17), while ligase III utilizes an alternative start site to produce a protein with and without a mitochondrial targeting signal (25). Studies by Zheng et al. suggested that the hDna2 mitochondrial localization signal is present in the C terminus of the protein and that no canonical nuclear localization signal is present (44). Therefore, we do not know how hDna2 is alternatively targeted to the mitochondria and the nucleus. Although in our biochemical fractionations both hDna2 species correspond to an approximately 120-kDa protein, we cannot assume that the mitochondrial and nuclear variants are identical gene products. The observation that the consensus EGFP-tagged full-length hDna2 protein seems to be exclusively mitochondrion targeted (44) does not rule out the presence of a distinct but similar-sized isoform that would show robust nuclear targeting. It does, however, strengthen the notion that hDna2 is a bona fide mitochondrial protein. Nevertheless, careful biochemical fractionation with appropriate controls in our experiments clearly demonstrated the existence of an endogenous nuclear hDna2 protein, and RNAi-mediated knockdown resulted in a clear nuclear phenotype, leaving no doubt that hDna2 is present in both the mitochondrial and nuclear compartments.

Importantly, we now provide direct evidence that hDna2 functions analogously to its counterparts in yeast and *Xenopus* cells, where it participates in the maintenance of nuclear DNA stability. Here we demonstrate that hDna2 depletion leads to reduced cell growth, accumulation of aneuploid cells, and an increase in internuclear bridges. Interestingly, the appearance of aneuploid cells is reminiscent of the "cut" phenotype observed in *Schizosaccharomcyes pombe* mutants defective in DNA replication and the S-phase/DNA damage checkpoint, where cells with incompletely replicated genomes fail to respond to the cell cycle checkpoint and enter a defective mitosis, resulting in aberrant DNA content (41). The appearance of internuclear bridges in hDna2-depleted cells could also be ascribed to hDna2's putative role in DNA repair or telomere stability. In yeast, Dna2 is important for telomere maintenance (10, 38), and in mammalian cells, loss of proteins essential in telomere stability, including the single-strand telomere-binding protein Pot1, can lead to the formation of such structures (13, 39). Alternatively, the internuclear bridges that we observed could be the result of defective DNA repair. Indeed, in yeast it was shown that Dna2 plays an important role in 5′-end resection and subsequent DNA repair (26, 45). Further work will focus on determining whether hDna2 plays an important role in telomere maintenance, DNA replication, and/or DNA repair, like its yeast counterpart.

ACKNOWLEDGMENTS

We thank B. Van Houten for the mtDNA damage protocol, Emily Cheng for the MitoTracker reagent and helpful comments, S. Goffart for the detailed protocol and advice on mtDNA analysis by 2DNAGE, Elise Oster for technical assistance with the DNA damage assay, Avi Silver for DNA preparations, and members of the Stewart and Spelbrink laboratories for useful comments. We also thank Jason Weber for critical reading of the manuscript.

This work was supported by the Cancer Biology Pathway, the Siteman Cancer Center at Barnes-Jewish Hospital, and the Washington University School of Medicine in St. Louis (J.P.D.); the Children's Discovery Institute (S.A.S.); Academy of Finland grants 110463 and 108380 (P.M.); USPHS GM087666 and the Ellison Foundation (J.L.C.); Academy of Finland grants 110689 and 103213 and CoE funding (J.N.S.); the Sigrid Juselius Foundation (J.N.S.); and the Tampere University Hospital Medical Research Fund (9G072 and 9H079 to J.N.S.).

REFERENCES

1. **Akbari, M., T. Visnes, H. E. Krokan, and M. Otterlei.** 2008. Mitochondrial base excision repair of uracil and AP sites takes place by single-nucleotide insertion and long-patch DNA synthesis. DNA Repair (Amsterdam) **7:**605–616.
2. Reference deleted.
3. **Bradford, M. M.** 1976. A rapid and sensitive method for the quantitation of microgram quantities of protein utilizing the principle of protein-dye binding. Anal. Biochem. **72:**248–254.
4. **Brewer, B. J., and W. L. Fangman.** 1987. The localization of replication origins on ARS plasmids in S. cerevisiae. Cell **51:**463–471.
5. **Budd, M. E., and J. L. Campbell.** 1995. A yeast gene required for DNA replication encodes a protein with homology to DNA helicases. Proc. Natl. Acad. Sci. USA **92:**7642–7646.
6. **Budd, M. E., and J. L. Campbell.** 1997. A yeast replicative helicase, Dna2 helicase, interacts with yeast FEN-1 nuclease in carrying out its essential function. Mol. Cell. Biol. **17:**2136–2142.
7. **Budd, M. E., and J. L. Campbell.** 2000. The pattern of sensitivity of yeast dna2 mutants to DNA damaging agents suggests a role in DSB and postreplication repair pathways. Mutat. Res. **459:**173–186.
8. **Budd, M. E., C. C. Reis, S. Smith, K. Myung, and J. L. Campbell.** 2006. Evidence suggesting that Pif1 helicase functions in DNA replication with the Dna2 helicase/nuclease and DNA polymerase δ. Mol. Cell. Biol. **26:**2490–2500.
9. **Chattopadhyay, R., L. Wiederhold, B. Szczesny, I. Boldogh, T. K. Hazra, T. Izumi, and S. Mitra.** 2006. Identification and characterization of mitochondrial abasic (AP)-endonuclease in mammalian cells. Nucleic Acids Res. **34:**2067–2076.
10. **Choe, W., M. Budd, O. Imamura, L. Hoopes, and J. L. Campbell.** 2002. Dynamic localization of an Okazaki fragment processing protein suggests a novel role in telomere replication. Mol. Cell. Biol. **22:**4202–4217.
11. **Coffey, G., U. Lakshmipathy, and C. Campbell.** 1999. Mammalian mitochondrial extracts possess DNA end-binding activity. Nucleic Acids Res. **27:**3348–3354.
12. **Cooper, H. M., and J. N. Spelbrink.** 2008. The human SIRT3 protein deacetylase is exclusively mitochondrial. Biochem. J. **411:**279–285.
13. **de Lange, T.** 2005. Shelterin: the protein complex that shapes and safeguards human telomeres. Genes Dev. **19:**2100–2110.
14. **de Souza-Pinto, N. C., D. M. Wilson III, T. V. Stevnsner, and V. A. Bohr.** 2008. Mitochondrial DNA, base excision repair and neurodegeneration. DNA Repair (Amsterdam) **7:**1098–1109.
15. **Formosa, T., and T. Nittis.** 1999. *Dna2* mutants reveal interactions with Dna polymerase α and Ctf4, a Pol α accessory factor, and show that full Dna2 helicase activity is not essential for growth. Genetics **151:**1459–1470.
16. **Friedman, K. L., and B. J. Brewer.** 1995. Analysis of replication intermediates by two-dimensional agarose gel electrophoresis. Methods Enzymol. **262:**613–627.
17. **Futami, K., A. Shimamoto, and Y. Furuichi.** 2007. Mitochondrial and nuclear localization of human Pif1 helicase. Biol. Pharm. Bull. **30:**1685–1692.
18. **Garrido, N., L. Griparic, E. Jokitalo, J. Wartiovaara, A. M. van der Bliek, and J. N. Spelbrink.** 2003. Composition and dynamics of human mitochondrial nucleoids. Mol. Biol. Cell **14:**1583–1596.
19. **Goffart, S., H. M. Cooper, H. Tyynismaa, S. Wanrooij, A. Suomalainen, and J. N. Spelbrink.** 2009. Twinkle mutations associated with autosomal dominant progressive external ophthalmoplegia lead to impaired helicase function and in vivo mtDNA replication stalling. Hum. Mol. Genet. **18:**328–340.
20. **Hakonen, A. H., S. Goffart, S. Marjavaara, A. Paetau, H. Cooper, K. Mattila, M. Lampinen, A. Sajantila, T. Lonnqvist, J. N. Spelbrink, and A. Suomalainen.** 2008. Infantile-onset spinocerebellar ataxia and mitochondrial recessive ataxia syndrome are associated with neuronal complex I defect and mtDNA depletion. Hum. Mol. Genet. **17:**3822–3835.
21. **Hakonen, A. H., P. Isohanni, A. Paetau, R. Herva, A. Suomalainen, and T. Lonnqvist.** 2007. Recessive Twinkle mutations in early onset encephalopathy with mtDNA depletion. Brain **130:**3032–3040.
22. **Kang, H.-Y., E. Choi, S.-H. Bae, K.-H. Lee, B.-S. Gim, H.-D. Kim, C. Park, S. A. MacNeill, and Y.-S. Seo.** 2000. Genetic analyses of *Schizosaccharomyces pombe dna2*$^+$ reveal that dna2 plays an essential role in Okazaki fragment metabolism. Genetics **155:**1055–1067.
23. **Kim, J. H., H. D. Kim, G. H. Ryu, D. H. Kim, J. Hurwitz, and Y. S. Seo.** 2006. Isolation of human Dna2 endonuclease and characterization of its enzymatic properties. Nucleic Acids Res. **34:**1854–1864.
24. **Korhonen, J. A., M. Gaspari, and M. Falkenberg.** 2003. TWINKLE has 5′→3′ DNA helicase activity and is specifically stimulated by mitochondrial single-stranded DNA-binding protein. J. Biol. Chem. **278:**48627–48632.
25. **Lakshmipathy, U., and C. Campbell.** 1999. The human DNA ligase III gene encodes nuclear and mitochondrial proteins. Mol. Cell. Biol. **19:**3869–3876.
26. **Liao, S., T. Toczylowski, and H. Yan.** 2008. Identification of the Xenopus DNA2 protein as a major nuclease for the 5′→3′ strand-specific processing of DNA ends. Nucleic Acids Res. **36:**6091–6100.
27. **Liu, P., L. Qian, J. S. Sung, N. C. de Souza-Pinto, L. Zheng, D. F. Bogenhagen, V. A. Bohr, D. M. Wilson III, B. Shen, and B. Demple.** 2008. Removal of oxidative DNA damage via FEN1-dependent long-patch base excision repair in human cell mitochondria. Mol. Cell. Biol. **28:**4975–4987.
28. **Liu, Q., W. Choe, and J. L. Campbell.** 2000. Identification of the Xenopus laevis homolog of Saccharomyces cerevisiae DNA2 and its role in DNA replication. J. Biol. Chem. **275:**1615–1624.
29. **Masuda-Sasa, T., O. Imamura, and J. L. Campbell.** 2006. Biochemical analysis of human Dna2. Nucleic Acids Res. **34:**1865–1875.
30. **Nikali, K., A. Suomalainen, J. Saharinen, M. Kuokkanen, J. N. Spelbrink, T. Lonnqvist, and L. Peltonen.** 2005. Infantile onset spinocerebellar ataxia is caused by recessive mutations in mitochondrial proteins Twinkle and Twinky. Hum. Mol. Genet. **14:**2981–2990.
31. **Pinter, S. F., S. D. Aubert, and V. A. Zakian.** 2008. The *Schizosaccharomyces pombe* Pfh1p DNA helicase is essential for the maintenance of nuclear and mitochondrial DNA. Mol. Cell. Biol. **28:**6594–6608.
32. **Saharia, A., L. Guittat, S. Crocker, A. Lim, M. Steffen, S. Kulkarni, and S. A. Stewart.** 2008. Flap endonuclease 1 contributes to telomere stability. Curr. Biol. **18:**496–500.
33. **Santos, J. H., J. N. Meyer, B. S. Mandavilli, and B. Van Houten.** 2006. Quantitative PCR-based measurement of nuclear and mitochondrial DNA damage and repair in mammalian cells. Methods Mol. Biol. **314:**183–199.
34. **Sarzi, E., S. Goffart, V. Serre, D. Chretien, A. Slama, A. Munnich, J. N. Spelbrink, and A. Rotig.** 2007. Twinkle helicase (PEO1) gene mutation causes mitochondrial DNA depletion. Ann. Neurol. **62:**579–587.
35. **Spelbrink, J. N., F. Y. Li, V. Tiranti, K. Nikali, Q. P. Yuan, M. Tariq, S. Wanrooij, N. Garrido, G. Comi, L. Morandi, L. Santoro, A. Toscano, G. M. Fabrizi, H. Somer, R. Croxen, D. Beeson, J. Poulton, A. Suomalainen, H. T. Jacobs, M. Zeviani, and C. Larsson.** 2001. Human mitochondrial DNA deletions associated with mutations in the gene encoding Twinkle, a phage T7 gene 4-like protein localized in mitochondria. Nat. Genet. **28:**223–231.
36. **Stewart, S. A., B. Poon, J. B. Jowett, and I. S. Chen.** 1997. Human immunodeficiency virus type 1 Vpr induces apoptosis following cell cycle arrest. J. Virol. **71:**5579–5592.
37. **Thyagarajan, B., R. A. Padua, and C. Campbell.** 1996. Mammalian mitochondria possess homologous DNA recombination activity. J. Biol. Chem. **271:**27536–27543.
38. **Tomita, K., T. Kibe, H. Y. Kang, Y. S. Seo, M. Uritani, T. Ushimaru, and M. Ueno.** 2004. Fission yeast Dna2 is required for generation of the telomeric single-strand overhang. Mol. Cell. Biol. **24:**9557–9567.
39. **Veldman, T., K. T. Etheridge, and C. M. Counter.** 2004. Loss of hPot1 function leads to telomere instability and a cut-like phenotype. Curr. Biol. **14:**2264–2270.
40. **Wanrooij, S., S. Goffart, J. L. Pohjoismaki, T. Yasukawa, and J. N. Spelbrink.** 2007. Expression of catalytic mutants of the mtDNA helicase Twinkle and polymerase POLG causes distinct replication stalling phenotypes. Nucleic Acids Res. **35:**3238–3251.
41. **Yanagida, M.** 1998. Fission yeast cut mutations revisited: control of anaphase. Trends Cell Biol. **8:**144–149.
42. **Yasukawa, T., M. Y. Yang, H. T. Jacobs, and I. J. Holt.** 2005. A bidirectional origin of replication maps to the major noncoding region of human mitochondrial DNA. Mol. Cell **18:**651–662.
43. **Zeviani, M., N. Bresolin, C. Gellera, A. Bordoni, M. Pannacci, P. Amati, M. Moggio, S. Servidei, G. Scarlato, and S. DiDonato.** 1990. Nucleus-driven multiple large-scale deletions of the human mitochondrial genome: a new autosomal dominant disease. Am. J. Hum. Genet. **47:**904–914.
44. **Zheng, L., M. Zhou, Z. Guo, H. Lu, L. Qian, H. Dai, J. Qiu, E. Yakubovskaya, D. F. Bogenhagen, B. Demple, and B. Shen.** 2008. Human DNA2 is a mitochondrial nuclease/helicase for efficient processing of DNA replication and repair intermediates. Mol. Cell **32:**325–336.
45. **Zhu, Z., W.-H. Chung, E. Y. Shim, S. E. Lee, and G. Ira.** 2008. Sgs1 helicase and two nucleases Dna2 and Exo1 resect DNA double-strand break ends. Cell **134:**981–994.